Biochemical and Biophysical Research Communications 434 (2013) 879–884

Contents lists available at SciVerse ScienceDirect

Biochemical and Biophysical Research Communications

journal homepage: www.elsevier.com/locate/ybbrc

Menadione and ethacrynic acid inhibit the hypoxia-inducible factor (HIF) pathway by disrupting HIF-1α interaction with p300

Yu-Ran Na [a], Ki-Cheol Han [a], Hyunsung Park [b], Eun Gyeong Yang [a,*]

[a] Center for Theragnosis, Biomedical Research Institute, Korea Institute of Science and Technology, Hwarangno 14-gil 5, Seongbuk-gu, Seoul 136-791, Republic of Korea
[b] Department of Life Science, University of Seoul, Siripdae-gil 13, Dongdaemun-gu, Seoul 130-743, Republic of Korea

ARTICLE INFO

Article history:
Received 2 April 2013
Available online 22 April 2013

Keywords:
Hypoxia inducible factor-1α
p300
Small molecule inhibitor
Menadione
Ethacrynic acid

ABSTRACT

Hypoxia is a general characteristic of most solid malignancies and intimately related to neoplastic diseases and cancer progression. Homeostatic response to hypoxia is primarily mediated by hypoxia inducible factor (HIF)-1α that elicits transcriptional activity through recruitment of the CREB binding protein (CBP)/p300 coactivator. Targeted blockade of HIF-1α binding to CBP/p300 would thus constitute a novel approach for cancer treatment by suppressing tumor angiogenesis and metastasis. Here, we identified inhibitors against the interaction between HIF-1α and p300 by a fluorescence polarization-based assay employing a fluorescently-labeled peptide containing the C-terminal activation domain of HIF-1α. Two small molecule inhibitors, menadione (MD) and ethacrynic acid (EA), were found to decrease expression of luciferase under the control of hypoxia-responsive elements in hypoxic cells as well as to efficiently block the interaction between the full-length HIF-1α and p300. While these compounds did not alter the expression level of HIF-1α, they down-regulated expression of a HIF-1α target vascular endothelial growth factor (VEGF) gene. Considering hypoxia-induced VEGF expression leading to highly aggressive tumor growth, MD and EA may provide new scaffolds for development of tumor therapeutic reagents as well as tools for a better understanding of HIF-1α-mediated hypoxic regulation.

1. Introduction

Low oxygen tension is prevalent in most solid tumor development [1,2]. Adaptation of cancer cells to hypoxia is critical for survival and growth and is mediated through the transcriptional activation of genes involved in tumor angiogenesis, metastasis, progression and glucose homeostasis [3–5]. Such cellular response is mainly orchestrated by the master switch hypoxia inducible factor-1α (HIF-1α). Under normoxic conditions, HIF-1α is hydroxylated on proline residues 402 and 564 by O_2-dependent prolyl hydroxylases (PHDs), followed by specific recognition by von Hippel-Lindau (VHL) and subsequent proteosomal degradation [6,7]. Under hypoxia, HIF-1α cannot be hydroxylated and thus rapidly accumulates. The stabilized HIF-1α is translocated to the nucleus, where it heterodimerizes with the β subunit [8,9]. Upon binding to the cognate DNA sequence, hypoxia response element (HRE), the heterodimer recruits the transcriptional coactivator CREB binding protein (CBP)/p300 to initiate transcription of hypoxia related genes such as vascular endothelial growth factor (VEGF), matrix metalloproteinase and lysyl oxidase [10–13].

Given the centrality of the HIF pathway in the cellular adaptation to hypoxia, inhibition of HIF function using novel inhibitors is an attractive therapeutic strategy for cancer treatment. Previous studies have validated that inhibition of the HIF pathway resulted in tumor regression [14,15], and several small molecule inhibitors have been discovered to disrupt the HIF pathway via a variety of molecular mechanisms including the inhibition of HIF-1α protein synthesis, stabilization, nuclear translocation and transactivation [16–19]. In addition, many anti-cancer agents under preclinical evaluation or clinical development were found to interfere with the HIF pathway indirectly [20–22].

The transcriptional activation of genes by HIF-1α is well characterized in structural studies [23,24]. HIF-1α recruits CBP/p300 through the direct interaction between the C-terminal activation domain (C-TAD) of HIF-1α and the cysteine/histidine rich domain 1 (CH1) of p300, which is critical for transcriptional activity of HIF-1α [23,24]. Furthermore, it has been reported that blockade of the HIF-1α-p300 interaction significantly attenuated HIF activity [19,25,26]. Hence, targeting the C-TAD-p300/CH1 interaction would provide an ideal strategy for blocking the HIF pathway. In the present report, we describe the discovery of new small molecule inhibitors against the HIF-1α-p300 interaction. Employing a fluorescence polarization (FP)-based assay and a cell-based HRE-dependent luciferase reporter assay, we screened a chemical library. As a result, menadione (MD) and ethacrynic acid (EA) were identified as effective inhibitors for the interaction of HIF-1α with p300 in vitro and in cellular levels, and were further found to re-

* Corresponding author. Fax: +82 2 958 5909.
E-mail address: eunyang@kist.re.kr (E.G. Yang).

0006-291X/$ - see front matter © 2013 Elsevier Inc. All rights reserved.
http://dx.doi.org/10.1016/j.bbrc.2013.04.044

duce the mRNA expression level of VEGF, one of the downstream target genes of HIF-1α.

2. Materials and methods

2.1. Materials

Human HeLa cervical epithelium cells (CCL-2) were purchased from the American Type Culture Collection (Manassas, VA, USA) and cultured in DMEM supplemented with 10% fetal bovine serum (Life Technologies, Grand Island, NY, USA). The cells were made hypoxic by incubating in a hypoxic incubator (Thermo Scientific, Waltham, MA, USA) at 37 °C. Chetomin (CTM), MD, EA and desferrioxamine (DFO) mesylate were obtained from Sigma–Aldrich (St. Louis, MO, USA). Anti-β-actin was purchased from Sigma–Aldrich, and anti-HIF-1α from BD Bioscience (San Jose, CA, USA). A fluorescein-labeled peptide containing amino acids 786–826 of HIF-1α CTAD denoted as F-786–826 was synthesized by conjugating fluorescein with the N-terminal insertion of an aminocaproic acid linker (AnyGen, KwangJu, Korea). All other chemicals were of the highest grade of purity commercially available.

2.2. Inhibitor screening

National Institute of Neurological Disorders and Stroke (NINDS) Custom Collection II (MicroSource Discovery Systems, Gaylordsville, CT, USA) was used to screen potential inhibitors against the interaction between HIF-1α and p300. An FP-based interaction assay was performed using GST-p300/CH1 and the F-786–826 peptide as described previously [22]. 100 nM of F-786–826 was incubated with 1.5 μM of GST-p300 in EBC buffer (50 mM Tris–HCl, pH 8.0, 120 mM NaCl, 0.25% Nonidet P-40, and 1 mM DTT) containing 40 μM chemicals at 25 °C. FP was then measured by an Appliskan multimode microplate reader (Thermo Scientific, Waltham, MA, USA) with an excitation/emission filter set of 485/535 nm.

2.3. Luciferase reporter assay

Luciferase reporter assays were performed as described previously [23]. Briefly, cells were plated in 24-well plates at a density of 5×10^4 cells/well. After attachment, cells were transfected with 200 ng of hypoxia reporter plasmid $p(HRE)_4$-Luc containing four copies of erythropoietin HRE and 50 ng of plasmid pCHO110 for β-galactosidase using Lipofectamine (Life Technologies) according to the manufacturer's instruction. Cells were treated with compounds at a final concentration of 20 μM, and vehicle samples were treated with culture media containing 0.1% DMSO. After incubation for 16 h, hypoxia was induced by incubating cells in a hypoxic incubator for 16 h. Cell extracts were prepared and analyzed using the Luciferase Assay System (Promega, Fitchburg, WI, USA). Measured luciferase activities were normalized by total protein concentrations which were determined by the Bradford assay (BioRad Laboratories, Hercules, CA, USA).

2.4. Determination of inhibitory activity of compounds

190 μL of p300/CH1 at a final concentration of 250 nM were incubated with varying concentrations of compounds in EBC buffer for 2 h at 25 °C, followed by addition of 10 μL of F-786–826 at a final concentration of 100 nM. FP values were then measured at 25 °C, and IC_{50} values for compounds were determined by nonlinear regression with sigmoidal dose–response curves using Sigmaplot software. All assays were performed in triplicate.

2.5. Recombinant protein expression and protein–protein interaction assay

DNA encoding CH1 of p300 (amino acids 300–520) were subcloned into pGEX-4T-1 (GE Healthcare, Little Chalfont, UK) or pET-28a (EMD Millipore, Billerica, MA, USA). His-p300/CH1 and GST-p300/CH1 were overexpressed and purified using Ni–NTA Sepharose and glutathione-Sepharose resins (Qiagen, Venlo, NED), respectively. Concentrations of the recombinant proteins were determined by the Bradford assay. Nuclear extracts were prepared from HeLa cells grown to high density in 100 mm dish, followed by purification using the nuclear extraction kit (EMD Millipore). To mimic hypoxia, HeLa cells were treated with 150 μM of DFO for 18 h. The protein concentrations of the nuclear extracts were determined by the Bradford assay. For the protein–protein interaction assay, 5 μg of His-p300/CH1 was incubated with 20 μL of Ni–NTA Sepharose in binding buffer (150 mM Tris–HCl pH 8.0, 360 mM NaCl, and 20 mM imidazole) at 4 °C for 2 h. Immobilized His-tagged proteins were incubated with varying concentrations of compounds at 4 °C for 2 h, followed by incubation with 50 μg of nuclear extracts at 4 °C for 2 h. After washing with the same buffer, the complexes were separated by SDS–PAGE and visualized by immunoblotting with monoclonal anti-HIF-1α (BD Bioscience, Franklin Lakes, NJ, USA). His-p300/CH1 proteins were visualized by Coomassie Brilliant Blue staining.

2.6. cell viability assay

HeLa cells were plated in 96-well plates at a density of 1×10^4 cells/well. After overnight incubation, cells were treated without (vehicle sample) or with varying concentrations of compounds for 16 h. All samples contained a final concentration of 0.5% DMSO (v/v). Cell viability was determined using an MTT cell viability reagent (Sigma–Aldrich). GI_{50} values were calculated by fitting the averages of triplicate measurements to sigmoid dose–response curves using Sigmaplot software.

2.7. Immunoblotting

HeLa cells were seeded in 6-well culture dishes at a density of 2×10^6 cells/well. After attachment, cells were treated with 0.1% DMSO, CTM (200 nM), MD (20 μM) or EA (50 μM) in media for 4 h, followed by incubation for an additional 16 h under normoxic or hypoxic (1% O_2) conditions. Cells were then lysed and the protein concentrations were determined by the Bradford assay. For immunoblotting, whole cell lysates were resuspended in SDS sample buffer, boiled for 5 min and run on SDS–PAGE gels, followed by transfer of the proteins to nitrocellulose membranes by semi-dry transfer (Trans-Blot SD, Bio-Rad). Proteins were reacted with anti-human HIF-1α antibody and/or with anti-β-actin antibody, and visualized by enhanced chemiluminescence according to the manufacturer's instruction (Pierce), with anti-mouse IgG conjugated with horseradish peroxidase as a secondary antibody.

2.8. Quantitative real-time PCR

HeLa cells (2×10^5 cells/well in 6-well plates) were treated with compounds for 16 h under normoxic or hypoxic (1% O_2) conditions. Total mRNA was extracted from HeLa cells using RNeasy Mini Kit (Qiagen). cDNA was synthesized from total RNA by using Maxime RT-PCR premix (Intron biotechnology, Seongnam, Korea). The primers for human VEGF and α-tubulin were designed as reported previously [24,25]: human VEGF (GenBank accession No.M32977) (forward: 5′-GCCTTGCTGCTCTACCTC-3′, reverse: 5′-GGCACACAGGATGGCTTG-3′); human α-tubulin (GenBank accession No. BC009314) (forward: 5′-AGCGTGCCTTTGTTCACTG-3′, re-

verse: 5′-CACACCAACCTCCTCATAATCC-3′). Quantitative PCRs were performed in triplicate on a Real-Time PCR system (Life Technologies) using SYBR Green PCR reagents. The mRNA expression of VEGF was normalized to that of α-tubulin, and relative quantification was performed according to the ΔΔCt method.

3. Results and discussion

3.1. Screening for inhibitors against the interaction of HIF-1α with p300

To discover novel small molecules that inhibit the interaction of HIF-1α with p300, we have optimized the previously developed FP-based assay in a 96-well plate format using a fluorescein-labeled CTAD peptide containing amino acids 786–826 of HIF-1α [22], which is critical for p300 binding [26]. 1040 FDA-approved drugs and bioactive compounds in NINDS custom collection II were then subjected to primary screening for their ability to inhibit the interaction of the F-786–826 peptide with GST-p300/CH1. With the threshold of 60% inhibition, six compounds were identified as initial hit candidates from the compound library (Fig. 1A). These compounds were then re-evaluated in secondary screening for their potential to inhibit transcriptional activity of HIF-1α in HeLa cells under hypoxia by an HRE-dependent luciferase reporter assay. As shown in Fig. 1B, two compounds, MD and EA, significantly reduced the relative luciferase activity, while others dramatically increased the activity unexpectedly. Accordingly, MD and EA whose structures are presented in Fig. 2A were finally selected as the inhibitors of the HIF-1α-p300/CH1 interaction and investigated further for their inhibitory activities.

3.2. Quantitative evaluation of inhibitory effects of the compounds on the interaction between the CTAD peptide of HIF-1α and p300/CH1

We next quantitatively analyzed the inhibitory potency of MD and EA for the interaction of the HIF-1α 786–826 peptide with p300/CH1 using the FP-based assay. CTM which is known as a direct disruptor of the HIF-1α-p300 interaction [27] was also included as a positive control in our experiments. When F-786–826 was incubated with GST-p300/CH1 in the presence of these compounds, FP values were observed to decrease in an incubation time-dependent manner to varying degrees (data not shown). In addition, pretreatment of GST-p300/CH1 with the compounds appeared to be critical to yield stable FP values. Therefore, GST-p300/CH1 was preincubated with each compound for 2 h, followed by addition of F-786–826. As shown in Fig. 2B, the % values for the interaction of F-786–826 with p300/CH1 decreased with increasing concentrations of the compounds. When their half maximal inhibitory concentration (IC_{50}) values were determined by nonlinear curve fitting, CTM showed an IC_{50} value of 651.7 ± 10.5 nM, which is consistent with the previously reported IC_{50} value of 540 ± 180 nM [28]. MD and EA had IC_{50} values of 9.2 ± 1.2 μM and 131.1 ± 5.8 μM, respectively. These data showed that MD and EA inhibited the HIF-1α peptide interaction with p300/CH1 approximately 14- and 200-fold less effectively than CTM. While hill slopes for MD (1.32) and EA (1.28) were closely similar, a hill slope of 3.73 for CTM was much higher, implying disparate inhibitory mechanisms of action. The mode of inhibition operated by CTM has previously been suggested to involve zinc ion ejection from the CH1 domain of p300 [27]. Although MD and EA likely exert inhibitory effects by acting on the p300 protein, the exact molecular mechanisms of MD and EA remain to be clarified.

3.3. Inhibitory activity of the compounds toward the interaction of p300/CH1 with the full length HIF-1α in vitro

Since the interaction of HIF-1α with its binding partner molecules was shown to be significantly affected by the length of HIF-1α fragments [29,30], the FP-based assay results based on the HIF-1α peptide might not reflect the true protein–protein interaction. Accordingly, we investigated whether MD and EA could inhibit the interaction of the full-length HIF-1α with p300 by a pull-down assay. In this experiment, His-p300/CH1 was used instead of GST-p300/CH1 because CTM significantly interfered with the interaction between glutathione on the surface of the Sepharose resin and GST during the assays (data not shown). Nuclear extracts containing the full-length HIF-1α was prepared from HeLa cells cultured in the presence of 150 μM DFO to mimic hypoxic conditions. Compound concentration ranges were selected based on the IC_{50} values obtained for the interaction of the HIF-1α peptide with p300/CH1. As shown in Fig. 3, the full-length HIF-1α was successfully pulled down by the His-p300/CH1 immobilized on the Ni–NTA resin and the amount of captured HIF-1α decreased with increasing concentrations of chemicals in a dose-dependent man-

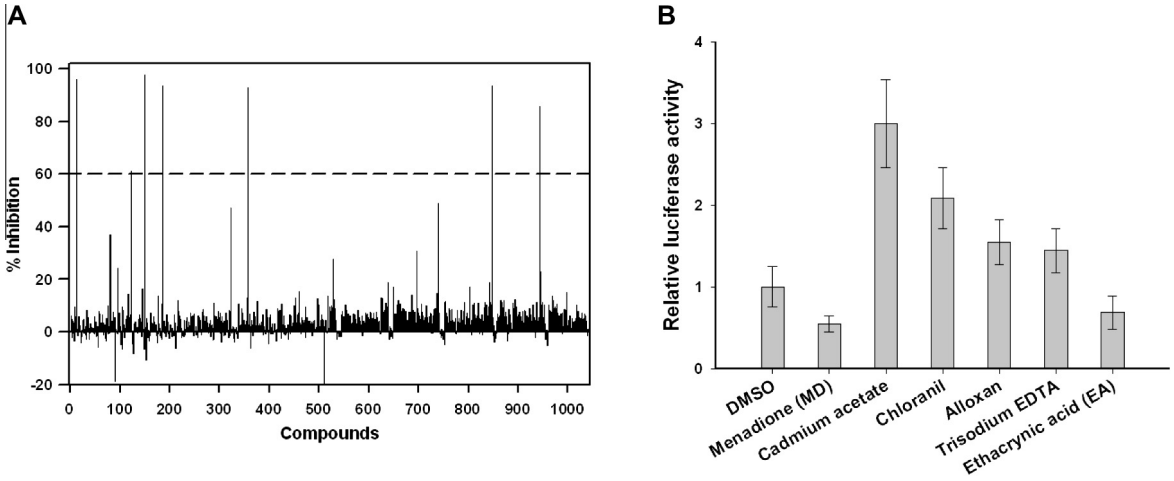

Fig. 1. Screen for inhibitors against the interaction of HIF-1α with p300. (A) An FDA-approved NINDS library containing 1040 compounds was screened using an FP-based interaction assay. F-786–826 at 100 nM was incubated with 1.5 μM of GST-p300/CH1 in EBC buffer in the presence of 40 μM chemicals at 25 °C, followed by FP measurements. The percentage of inhibition was calculated and presented with a dotted line at 60% inhibition. (B) HeLa cells were transfected with both $p(HRE)_4$-luc and pCHO110, followed by culturing in the presence of inhibitory compound candidates under hypoxic conditions for 16 h. Relative luciferase activities were normalized with that of the DMSO vehicle control. Each bar represents the average of triplicate assays ± SD.

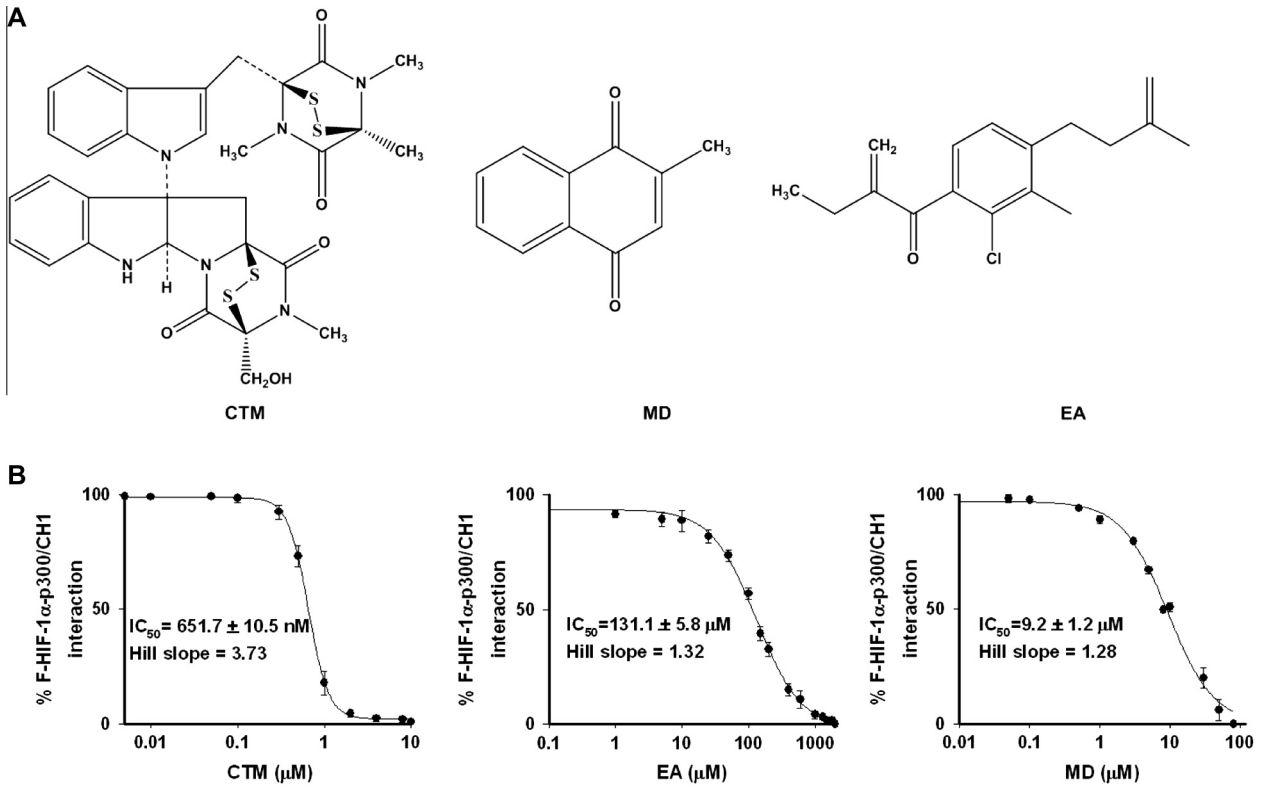

Fig. 2. (A) Structures of the inhibitory compounds, CTM, MD and EA. (B) FP-based interaction assay. F-786–826 was bound to GST-p300/CH1 in the presence of varying concentrations of compounds. Each data point represents the average of triplicate assays ± SD.

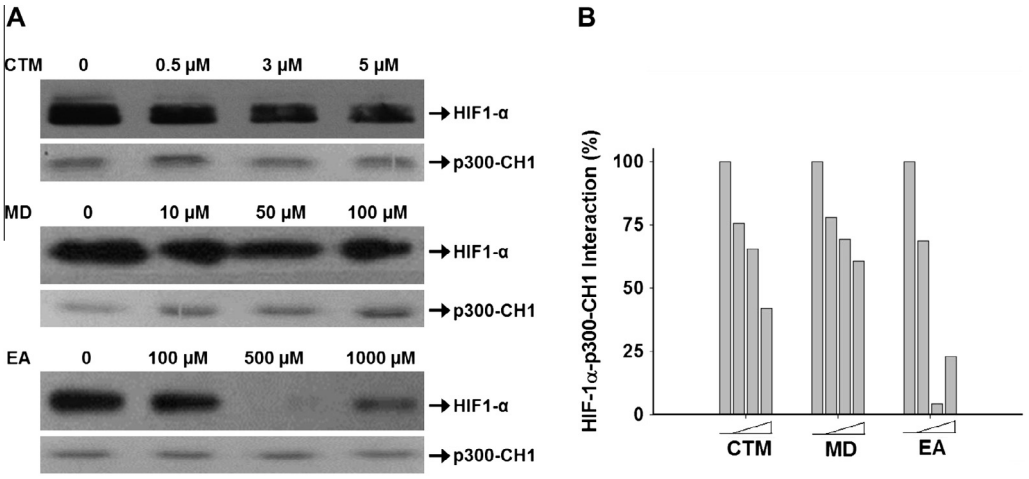

Fig. 3. Effects of CTM, MD and EA on the interaction between p300/CH1 and the full-length HIF-1α in vitro. (A) Co-immunoprecipitation of His-p300/CH1 bound HIF-1α at indicated concentrations of compounds. His-p300/CH1 proteins were incubated with varying concentrations of compounds, followed by incubation with nuclear extracts prepared from HeLa cells treated with DFO. Complexes were analyzed by immunoblotting using anti-HIF-1α antibody or Coomassie staining to detect His-p300/CH1. (B) Quantitation of the co-immunoprecipitation data. HIF-1α band intensities were normalized to the level of the vehicle sample.

ner. This result is in accordance with the data from the FP-based assay, demonstrating clearly that MD and EA can effectively inhibit the interaction between p300/CH1 and the endogenous full-length HIF-1α.

3.4. Biological activities of the compounds

After we confirmed that MD and EA inhibit the interaction of HIF-1α with p300/CH1, we examined whether these compounds could block the HIF pathway to result in down-regulation of VEGF expression. Prior to evaluating the compounds in cell culture assays, we tested their effects on cell viability to determine the concentrations at which cellular changes due to cytotoxicity would be minimal. An MTT assay was performed for HeLa cells treated with CTM over a concentration range from 30 nM to 10 μM, whereas MD and EA were used from 0.5 μM to 900 μM. As shown in Fig. 4A, the survival was dependent on the dose of the compounds, eventually approaching zero. The calculated GI_{50} values for CTM, MD and EA were 861.3 ± 29.7 nM, 40.6 ± 3.2 μM and 234.4 ± 6.5 μM, respectively. These results showed conclusively that MD and EA are considerably less toxic than CTM to HeLa cells. In addition, these GI_{50} values were used to determine the upper

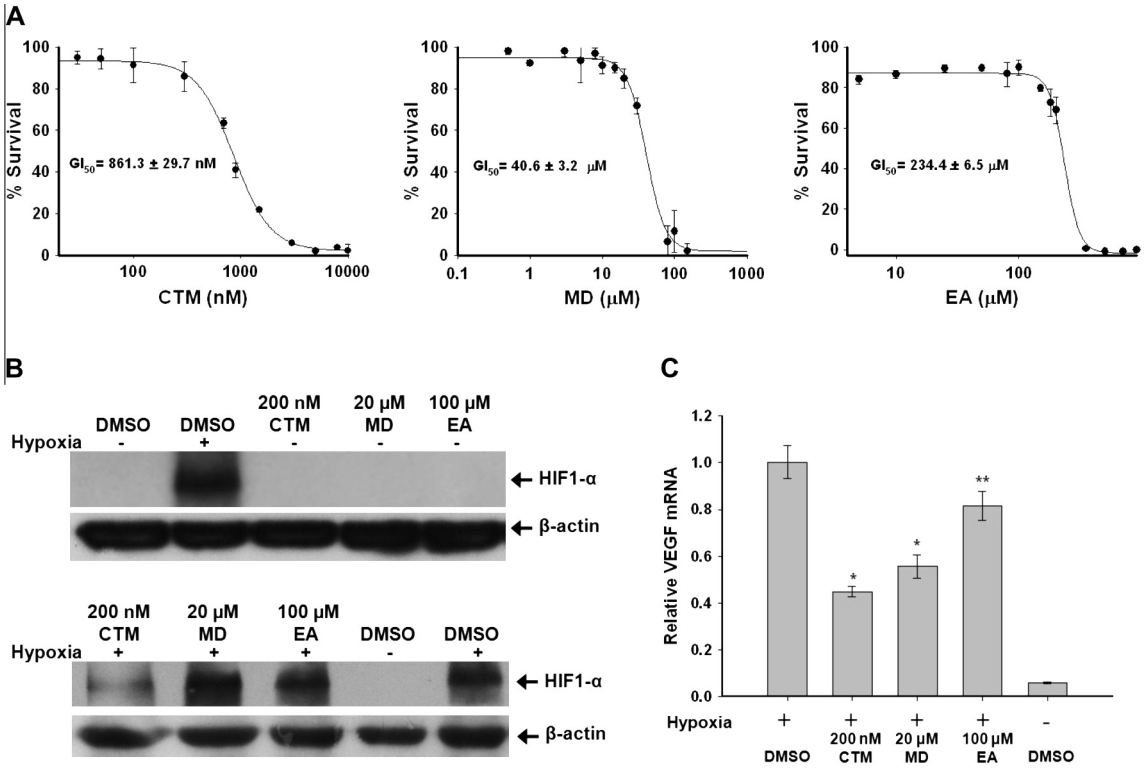

Fig. 4. Effects of CTM, MD and EA on cell survival, HIF-1α expression, and VEGF transcription. (A) Cell viability was determined following treatment with compounds for 16 h. All samples contained 0.5% DMSO as a vehicle. Each data point represents the average of triplicate assays ± SD. (B) Western blot analysis of HIF-1α levels in cells treated with compounds at the indicated concentrations for 16 h under normoxic (20% O_2) or hypoxic (1% O_2) conditions. (C) Quantitative real-time PCR analysis of VEGF gene expression. HeLa cells were treated with CTM, MD and EA at the indicated concentrations for 16 h under normoxic (20% O_2) or hypoxic (1% O_2) conditions. The relative amount of VEGF mRNA normalized to that of normoxic cells was expressed as an arbitrary unit. Each bar represents the average of three independent assays ± SD. $^{*}p < 0.005$ and $^{**}p < 0.02$.

concentration limits for evaluating the compounds in cell based assays.

We next investigated the effects of the compounds on the stability of HIF-1α in HeLa cells by Western blot analysis. As expected, HIF-1α was not detected under the normoxic condition, whereas the expression of HIF-1α under hypoxia was enhanced irrespective of the presence of MD or EA within the ranges without cytotoxicity (Fig. 4B). This result indicated that MD and EA did not affect endogenous HIF-1α expression levels stabilized by hypoxic treatment of HeLa cells. However, it should be noted that CTM decreased abundance of hypoxia-stabilized HIF-1α significantly (Fig. 4B), which is inconsistent with the previous study using Hep3B cells [31].

To address the inhibitory effect of the compounds on the transcriptional activity of HIF-1α, VEGF mRNA levels were analyzed in HeLa cells under hypoxic conditions by quantitative real-time PCR because VEGF is one of the downstream targets of the HIF-1α pathway and a particularly attractive target for anticancer therapy due to its important role in pathological angiogenesis in most types of cancers [32]. As shown in Fig. 4C, elevated VEGF mRNA levels in hypoxic cells were attenuated in the presence of MD and EA as well as CTM although MD had a more dramatic inhibitory effect than EA. These results successfully demonstrated that MD and EA inhibit HIF-1α transcriptional activity at the cellular level.

The present study was designed to identify effective small molecule inhibitors for the HIF pathway through the disruption of HIF-1α-p300/CH1 interaction since inhibition of the HIF pathway can have profound therapeutic value for cancer treatment. We have discovered MD and EA as moderately potent small molecule inhibitors using an FP-based assay and an HRE-dependent luciferase reporter assay. Our data showed that MD and EA do not interfere with the expression level of HIF-1α, but efficiently inhibit the transcriptional activity of HIF on the target gene VEGF at the cellular level with disruption of the HIF-1α-p300 interaction. This demonstrated that disruption of the HIF-1α-p300 interaction by small molecules could lead to blockade of the HIF signal transduction pathway. Therefore, MD and EA could provide new scaffolds for the development of therapeutic reagents in tumor treatments as well as tools for the understanding of hypoxic regulation by the HIF pathway.

Acknowledgments

This work was supported by the Proteogenomics Research Program funded by the Korean Ministry of Education, Science and Technology, and by the KIST grant.

References

[1] P. Vaupel, O. Thews, D.K. Kelleher, M. Hoeckel, Current status of knowledge and critical issues in tumor oxygenation. Results from 25 years research in tumor pathophysiology, Adv. Exp. Med. Biol. 454 (1998) 591–602.
[2] P. Vaupel, K.H. Schlenger, M. Hoeckel, P. Okunieff, Oxygenation of mammary tumors: from isotransplanted rodent tumors to primary malignancies in patients, Adv. Exp. Med. Biol. 316 (1992) 361–371.
[3] G.U. Dachs, G.M. Tozer, Hypoxia modulated gene expression: angiogenesis, metastasis and therapeutic exploitation, Eur. J. Cancer 36 (2000) 1649–1660.
[4] A.C. Koong, N.C. Denko, K.M. Hudson, C. Schindler, L. Swiersz, C. Koch, S. Evans, H. Ibrahim, Q.T. Le, D.J. Terris, A.J. Giaccia, Candidate genes for the hypoxic tumor phenotype, Cancer Res. 60 (2000) 883–887.
[5] M. Hockel, P. Vaupel, Tumor hypoxia: definitions and current clinical, biologic, and molecular aspects, J. Natl. Cancer Inst. 93 (2001) 266–276.
[6] L.E. Huang, J. Gu, M. Schau, H.F. Bunn, Regulation of hypoxia-inducible factor 1alpha is mediated by an O_2-dependent degradation domain via the ubiquitin-proteasome pathway, Proc. Natl. Acad. Sci. USA 95 (1998) 7987–7992.
[7] M. Ivan, K. Kondo, H. Yang, W. Kim, J. Valiando, M. Ohh, A. Salic, J.M. Asara, W.S. Lane, W.G. Kaelin Jr., HIFalpha targeted for VHL-mediated destruction by proline hydroxylation: implications for O_2 sensing, Science 292 (2001) 464–468.

[8] L.E. Huang, H.F. Bunn, Hypoxia-inducible factor and its biomedical relevance, J. Biol. Chem. 278 (2003) 19575–19578.
[9] C.W. Pugh, P.J. Ratcliffe, Regulation of angiogenesis by hypoxia: role of the HIF system, Nat. Med. 9 (2003) 677–684.
[10] G. Semenza, Signal transduction to hypoxia-inducible factor 1, Biochem. Pharmacol. 64 (2002) 993–998.
[11] R. Roskoski Jr., Vascular endothelial growth factor (VEGF) signaling in tumor progression, Crit. Rev. Oncol. Hematol. 62 (2007) 179–213.
[12] J.T. Erler, K.L. Bennewith, M. Nicolau, N. Dornhofer, C. Kong, Q.T. Le, J.T. Chi, S.S. Jeffrey, A.J. Giaccia, Lysyl oxidase is essential for hypoxia-induced metastasis, Nature 440 (2006) 1222–1226.
[13] D. Liao, R.S. Johnson, Hypoxia: a key regulator of angiogenesis in cancer, Cancer Metastasis Rev. 26 (2007) 281–290.
[14] L. Li, X. Lin, M. Staver, A. Shoemaker, D. Semizarov, S.W. Fesik, Y. Shen, Evaluating hypoxia-inducible factor-1alpha as a cancer therapeutic target via inducible RNA interference in vivo, Cancer Res. 65 (2005) 7249–7258.
[15] S. Yin, S. Kaluz, N.S. Devi, A.A. Jabbar, R.G. de Noronha, J. Mun, Z. Zhang, P.R. Boreddy, W. Wang, Z. Wang, T. Abbruscato, Z. Chen, J.J. Olson, R. Zhang, M.M. Goodman, K.C. Nicolaou, E.G. Van Meir, Arylsulfonamide KCN1 Inhibits In Vivo Glioma Growth and Interferes with HIF Signaling by Disrupting HIF-1alpha Interaction with Cofactors p300/CBP, Clin. Cancer. Res. 18 (2012) 6623–6633.
[16] L.P. Liu, R.L. Ho, G.G. Chen, P.B. Lai, Sorafenib inhibits hypoxia-inducible factor-1alpha synthesis: implications for antiangiogenic activity in hepatocellular carcinoma, Clin. Cancer. Res. 18 (2012) 5662–5671.
[17] A. Yamaki, H. Muratsubaki, Phenazine methosulfate decreases HIF-1alpha accumulation during the exposure of cells to hypoxia, Biosci. Biotechnol. Biochem. 76 (2012) 1682–1687.
[18] C.D. Befani, P.J. Vlachostergios, E. Hatzidaki, A. Patrikidou, S. Bonanou, G. Simos, C.N. Papandreou, P. Liakos, Bortezomib represses HIF-1alpha protein expression and nuclear accumulation by inhibiting both PI3K/Akt/TOR and MAPK pathways in prostate cancer cells, J. Mol. Med. (Berl) 90 (2012) 45–54.
[19] H.S. Kwon, D.R. Kim, E.G. Yang, Y.K. Park, H.C. Ahn, S.J. Min, D.R. Ahn, Inhibition of VEGF transcription through blockade of the hypoxia inducible factor-1alpha-p300 interaction by a small molecule, Bioorg. Med. Chem. Lett. 22 (2012) 5249–5252.
[20] P.J. Kallio, K. Okamoto, S. O'Brien, P. Carrero, Y. Makino, H. Tanaka, L. Poellinger, Signal transduction in hypoxic cells: inducible nuclear translocation and recruitment of the CBP/p300 coactivator by the hypoxia-inducible factor-1alpha, EMBO J. 17 (1998) 6573–6586.
[21] Z. Arany, L.E. Huang, R. Eckner, S. Bhattacharya, C. Jiang, M.A. Goldberg, H.F. Bunn, D.M. Livingston, An essential role for p300/CBP in the cellular response to hypoxia, Proc. Natl. Acad. Sci. USA 93 (1996) 12969–12973.
[22] H. Cho, D.R. Ahn, H. Park, E.G. Yang, Modulation of p300 binding by posttranslational modifications of the C-terminal activation domain of hypoxia-inducible factor-1alpha, FEBS Lett. 581 (2007) 1542–1548.
[23] H. Cho, H.Y. Lee, D.R. Ahn, S.Y. Kim, S. Kim, K.B. Lee, Y.M. Lee, H. Park, E.G. Yang, Baicalein induces functional hypoxia-inducible factor-1alpha and angiogenesis, Mol. Pharmacol. 74 (2008) 70–81.
[24] M.J. Lee, J.W. Kim, E.G. Yang, Hinokitiol activates the hypoxia-inducible factor (HIF) pathway through inhibition of HIF hydroxylases, Biochem. Biophys. Res. Commun. 396 (2010) 370–375.
[25] Y. Li, X. Zhou, M.A. St John, D.T. Wong, RNA profiling of cell-free saliva using microarray technology, J. Dent. Res. 83 (2004) 199–203.
[26] D. Lando, D.J. Peet, D.A. Whelan, J.J. Gorman, M.L. Whitelaw, Asparagine hydroxylation of the HIF transactivation domain a hypoxic switch, Science 295 (2002) 858–861.
[27] K.M. Cook, S.T. Hilton, J. Mecinovic, W.B. Motherwell, W.D. Figg, C.J. Schofield, Epidithiodiketopiperazines block the interaction between hypoxia-inducible factor-1alpha (HIF-1alpha) and p300 by a zinc ejection mechanism, J. Biol. Chem. 284 (2009) 26831–26838.
[28] K.M. Block, H. Wang, L.Z. Szabo, N.W. Polaske, L.K. Henchey, R. Dubey, S. Kushal, C.F. Laszlo, J. Makhoul, Z. Song, E.J. Meuillet, B.Z. Olenyuk, Direct inhibition of hypoxia-inducible transcription factor complex with designed dimeric epidithiodiketopiperazine, J. Am. Chem. Soc. 131 (2009) 18078–18088.
[29] P. Koivunen, M. Hirsila, V. Gunzler, K.I. Kivirikko, J. Myllyharju, Catalytic properties of the asparaginyl hydroxylase (FIH) in the oxygen sensing pathway are distinct from those of its prolyl 4-hydroxylases, J. Biol. Chem. 279 (2004) 9899–9904.
[30] D. Ehrismann, E. Flashman, D.N. Genn, N. Mathioudakis, K.S. Hewitson, P.J. Ratcliffe, C.J. Schofield, Studies on the activity of the hypoxia-inducible-factor hydroxylases using an oxygen consumption assay, Biochem. J. 401 (2007) 227–234.
[31] A.L. Kung, S.D. Zabludoff, D.S. France, S.J. Freedman, E.A. Tanner, A. Vieira, S. Cornell-Kennon, J. Lee, B. Wang, J. Wang, K. Memmert, H.U. Naegeli, F. Petersen, M.J. Eck, K.W. Bair, A.W. Wood, D.M. Livingston, Small molecule blockade of transcriptional coactivation of the hypoxia-inducible factor pathway, Cancer Cell 6 (2004) 33–43.
[32] N. Ferrara, Vascular endothelial growth factor as a target for anticancer therapy, Oncologist 9 (Suppl. 1) (2004) 2–10.